Available online at http://www.journalcra.com

International Journal of Current Research
Vol. 6, Issue, 03, pp.5743-5748, March, 2014

INTERNATIONAL JOURNAL OF CURRENT RESEARCH

ISSN: 0975-833X

RESEARCH ARTICLE

STUDY OF NANOCRYSTALLINE STRUCTURE AND MICRO PROPERTIES OF ZRO_2 POWDERS BY USING RIETVELD METHOD

[1*]Nabeel A. Bakr, [2]Tagreed. M. Al-Saadi and [1]Noor A. Hameed

[1]Department of Physics, College of Science, University of Diyala, Diyala, Iraq
[2]Department of Physics, College of Education for Pure Science, University of Baghdad, Baghdad, Iraq

ARTICLE INFO

Article History:
Received 14th December, 2013
Received in revised form
30th January, 2014
Accepted 19th February, 2014
Published online 25th March, 2014

Key words:
Rietveld method,
Fullprof,
Qualitative analysis,
XRD, ZrO_2 Powder.

ABSTRACT

In this study, we report the qualitative phase analysis performed by Rietveld X-ray diffraction using "Fullprof" program for nano and micro powder of ZrO_2 before and after heat treatment at (1180 °C). Rietveld refinement on X-ray data for the samples is performed. The obtained results have a good optimization between the observed X-ray diffraction pattern and that calculated by Rietveld method. This optimization is determined according to R-pattern factor (R_p), the weighted-profile factor (R_{wp}), and goodness of the fit (GOF). The particles morphology of the powder before and after heat treatment is identified using SEM. The final result shows that Rietveld refinement is more accurate than comparing method.

INTRODUCTION

Zirconium oxide (ZrO_2), sometimes known as zirconia, is an extremely important oxide because of its useful properties. Zirconia is one of the most important compounds in materials science and technology because it combines excellent mechanical, thermal, chemical, and dielectric properties: high melting point (2700 ^oC), low thermal and electronic conductivity, good oxygen-ion conductivity at elevated temperatures, high strength and enhanced fracture toughness, chemical inertness, and resistance to corrosion, high dielectric constant, wide band gap, heated zirconia can be utilized as a source of infrared radiation and white light, etc (Taylor *et al*., 2012; Garcia *et al*., 2012; Al-hazmi, 2005). Its properties depend mainly on the degree of stabilization, quantity of stabilizer and quality of the original raw material (Buckley, 2006). Ziniarco is used in a wide range of applications such as catalysts, oxygen sensors, fuel cells, engine parts, thermal barrier coatings on metal surfaces, high durability coating (Kazemi *et al*., 2011; Gateshki *et al*., 2006). ZrO_2 appears in three different polymorphs depending on pressure, temperature, impurity or doping content, growth conditions, etc are: monoclinic, tetragonal and cubic (Taylor *et al*., 2012). Pure zirconia is monoclinic at room temperature, (space group *P21 /c*), this phase is stable up to 1170°C (T < 1170 °C), above this temperature 1170 < T < 2370 °C) it transforms into tetragonal (space group *P42 /nmc*) and then into cubic phase (T > 2370 °C) (space group *Fm*3*m*) (Štefanić and Musić, 2002; Piconi and Maccauro, 1999; Foster *et al*., 2001; Abbas *et al*., 2008; Fabris *et al*., 2002).

***Corresponding author: Nabeel A. Bakr,** Department of Physics, College of Science, University of Diyala, Diyala, Iraq*

monoclini $\xrightarrow{1170°C}$ tetragonal $\xrightarrow{2370°C}$ cubic $\xrightarrow{2680°C}$ melt

Phase transformations between cubic and tetragonal, and tetragonal and monoclinic phases occur on cooling from high temperatures (Zhu *et al*., 2012). In this article we present characterization properties of nanocrystalline and microcrystalline structure of two commercially available ZrO_2 nano and micro powders).

Experimental Work

Materials

The structure investigations were performed on two commercial zirconia materials:

Commercial nanopowder (Hongwu Nanometer Co. Ltd., Reagent Grade, 40-50 nm, 99.9% purity).
Commercial micropowder (Hongwu Nanometer Co. Ltd., Reagent Grade, 70-80 nm, 99.9% purity).

Experimental Conditions

The collection of X-ray diffraction patterns was performed by the use of (Shimadzu XRD-6000) goniometer with copper

target (Cu K_α, 1.5406 Å), (40 kV, 30 mA). The samples were mounted on an aluminum sample holder. Step-scan data were collected from (20°-80°) with a step width of 0.02°. The time of data acquisition was chosen to obtain the intensity of the most intense diffraction line of 5 sec/step counts for all X-ray patterns. The divergence, scattering, and receiving slits are 1.0◦, 1.0◦ and 0.30 (mm) respectively. The Rietveld analysis was performed by applying Fullprof program.

Rietveld Analysis

Rietveld method can be defined as a crystal structure refinement method, from powder diffraction data. A pattern is calculated from a series of structural parameters (cell, atomic coordinates, thermal motion, etc), peak shape and width parameters (plus background, Lorentz-polarisation correction, etc), and compared to the observed data (Rietveld, 1969; Rietveld, 1967). Rietveld method can be used to solve a structure from the powder diffraction data. It starts by taking a trial structure, calculating a powder diffraction profile from it and then comparing it with the measured profile. The trial structure can then be gradually modified by changing the atomic positions and refined until a best-fit match with the measured pattern is obtained. The validity of the structure obtained is assessed by R factor, and by a difference plot of the two patterns (Smart and Moore, 2005). The basic idea behind the Rietveld method is the calculation of the entire powder pattern using a variety of different refinable parameters. The parameters can roughly be divided into three categories: structural parameters, which mainly affect the intensities of the Bragg reflections, profile parameters, which are determined by the instrument, the sample, and background parameters (Dinnebier and Friese, 2003). The Rietveld method uses a model to calculate a diffraction pattern which is then compared with observed data. The difference between all data set points of the observed and the calculated profiles is minimized by a least squares refinement of selected parameters. The least-squares refinement leads to a minimal residual quantity S_y (Ståhl, 2008; Snellings *et al*., 2010):

$$S_y = \sum_i w_i(Y_{oi} - Y_{ci})^2 \quad \text{…….. (1)}$$

Where Y_{oi} : is the observed intensity at point i of the observed powder pattern, Y_{ci} : is the calculated intensity for the i_{th} data point and w_i : The weight at point *i* in the diffraction profile which is based on the counting statistics. Many different statistical agreement factors have been proposed for judging the quality of a Rietveld refinement. The most common one is the so called weighted profile R-factor (R_{wp}). These factors measure not just how well the structural model fits the diffraction intensities, but also how well we have fit the background and how well the diffraction positions and peak shapes have been fit (Dinnebier and Friese, 2003; Toby, 2006). The calculated intensities y_{ci} are determined by summing the contributions from neighboring Bragg reflections plus the background (de Oliveira *et al*., 2006; Karolus, 2003):

$$Y_{ci} = S\sum_k L_k F_k Ø (2Θ_i-2Θ_k) O_k A + Y_{bi} \quad \text{…….. (2)}$$

Where S is the scale factor, K represents the Miller indices (hkl) for a Bragg's reflection (which depends on the symmetry), L_k is a function containing Lorentz, polarization and multiplicity factors, Ø the reflection profile function, O_k is the preferred orientation function, A is an is an absorption correction factor. (which depends on the thickness of the sample, diffraction geometry and actual weighted average linear absorption coefficient). It is constant throughout the pattern, and is normally included in the scale factor), F_k is the structure factor for (k^{th}) Bragg reflection and Y_{bi} is the background intensity at i^{th} step. At the end of a refinement it is necessary to check whether the results are meaningful, and whether they meet certain standard criteria through measure the agreement between the observed and calculated models. One of the ways to measure the agreement between the observed and calculated models is adjusting the various atomic parameters so that the calculated structure factors match the observed structure factors as closely as possible. The factors called (Reliability factors) sometimes called the agreement factors. There are several R values: R-structure factor (R_F), R-Bragg factor (R_B), R-pattern factor (R_p), the weighted-profile factor (R_{wp}) and the expected factor (R_{exp}) (Will, 2005; Saravanan and Rani, 2012).

1-Weighted-profile Reliability factors (Al-Dhahir, 2013; Mccusker *et al*., 1999)

$$R_{wp} = \sum_i W_i (y_{oi} - y_{ci})^2 / \sum_i W_i (y_{oi})^2 \quad \text{…….. (3)}$$

2-Expected Reliability factors (Porob *et al*., 2001)

$$R_{exp} = [(N - P) / \sum_i W_i (y_{oi})^2]^{1/2} \quad \text{…….. (4)}$$

3-The goodness of fit (χ^2) (Mccusker *et al*., 1999; Nowosielski *et al*., 2008)

$$\chi = [S_y / (N-P)]^{1/2}$$

$$\chi^2 = \sum_i w_i(Y_{i-} Y_{ci})^2 /(N-P) = R_{wp} / R_{exp} \quad \text{…….. (5)}$$

Where **N** is the number of observations and P is the number of parameters.

Williamson-Hall Method

Williamson-Hall method of the X-ray analysis is used for the precise determination of crystallite size distribution and analysis of lattice strains (Goforth *et al*., 2000).

The average crystalline size was calculated using Debye-Scherrer's formula (Mote *et al*., 20102; Zak *et al*., 2011; Rehani *et al*., 2006; Prabhu *et al*., 2013):

$$D = K\lambda / \beta_D \cos\Theta$$

where D crystalline size, K a constant whose value depends on particle shape, λ wavelength of Cu kα radiation and β_D is the broadening solely due to small crystallite size.

The strain induced in powders due to crystal imperfection and distortion was calculated using the formula:

$$\varepsilon = \beta_s / 4\tan\Theta$$

Where β_s is the peak broadening due to lattice strain, Θ is the Bragg's angle. From above two equations, it was confirmed

that the peak width from crystallite size varies as 1/cosΘ strain varies as tanΘ. Assuming that the particle size and the strain contributions to line broadening are independent to each other and both have a Cauchy-like profile, the total peak broadening β_{hkl} may be expressed as:

$$\beta_{hkl} = \beta_D + \beta_s$$

$$\beta_{hkl} \cos\Theta = (K\lambda / D) + (4\varepsilon \sin\Theta) \quad \ldots\ldots\ldots (6)$$

The above equations are W-H equations. A plot is drawn with sinΘ along the x-axis and β_{hkl} cosΘ along the y-axis.

RESULTS AND DISCUSSION

XRD patterns of all samples are shown in Figure (1). The patterns of ZrO_2 nanopowder (before heat treatment and after heat treatment) exhibited strong diffraction peaks at (28.297°, 31.586°, 50.251°) and (28.123°, 31.411°, 50.089°) respectively. While XRD patterns of ZrO_2 micro powder (before heat treatment and after heat treatment at 1180 °C) exhibited strong diffraction peaks at (28.223°, 31.485°, 50.206°) and (28.324°, 31.605°, 50.286°) respectively. Rietveld refinements of all ZrO_2 samples are shown in Figure (2). The experimental points are plotted as dots (.) and theoretical data (calculated by equation 2) are shown as solid line. The difference between theoretical and experimental data is shown in the bottom line of each figure. The vertical lines represent the Bragg's allowed peaks.

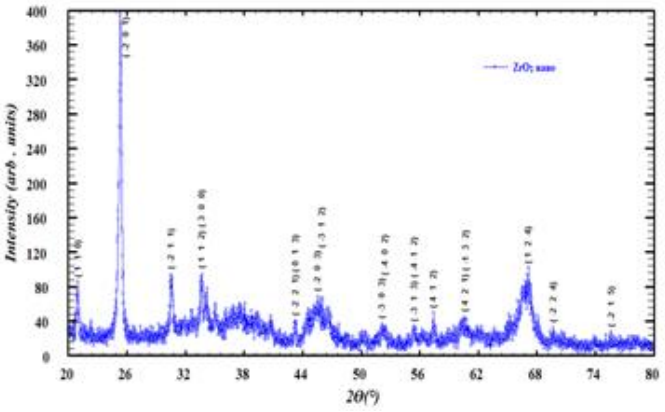

(a)

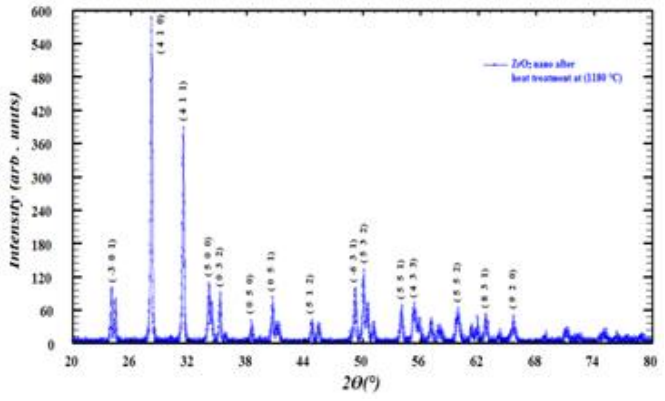

(b)

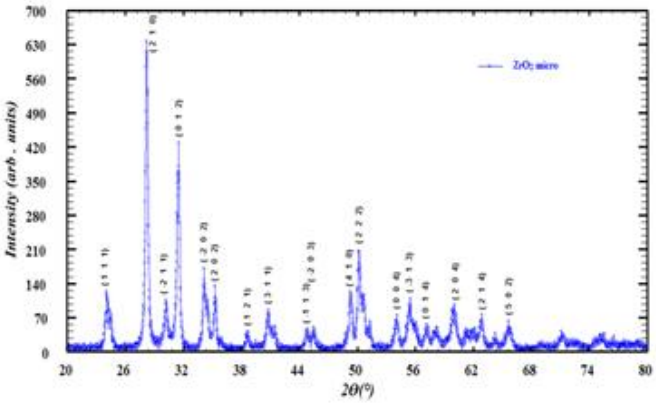

(c)

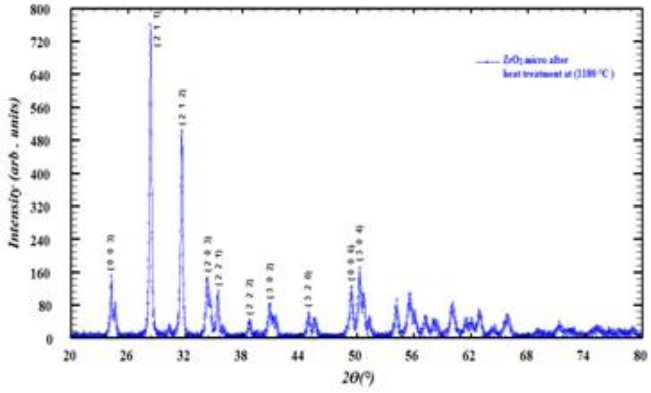

(d)

Figure 1. X-ray diffraction pattern of: (a) ZrO_2 nanopowder, (b) ZrO_2 nanopowder after heat treatment at (1180 °C), (c) ZrO_2 micropowder, (d) ZrO_2 micropowder after heat treatment at (1180 °C)

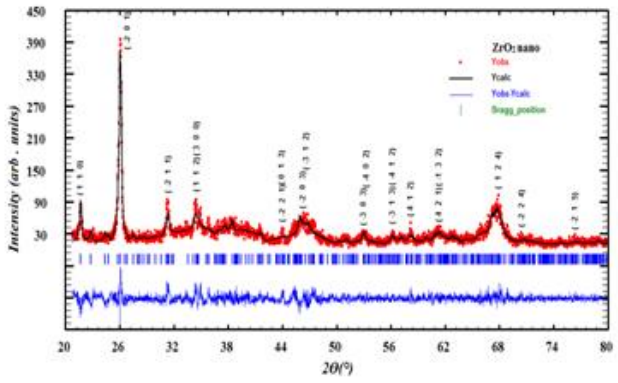

(a)

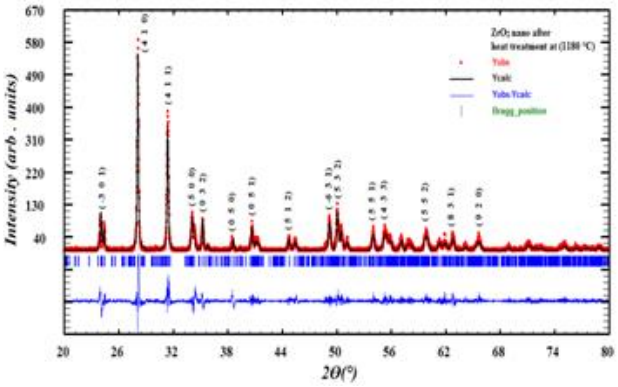

(b)

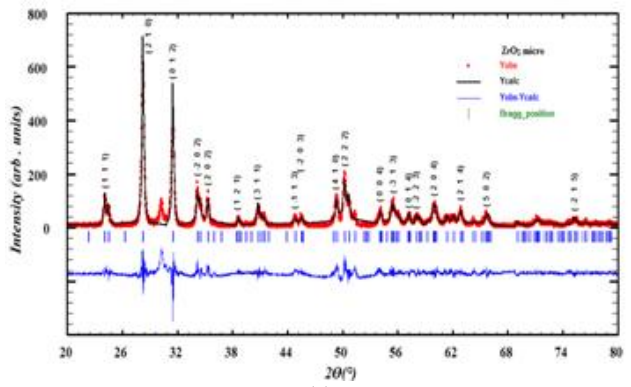

(c)

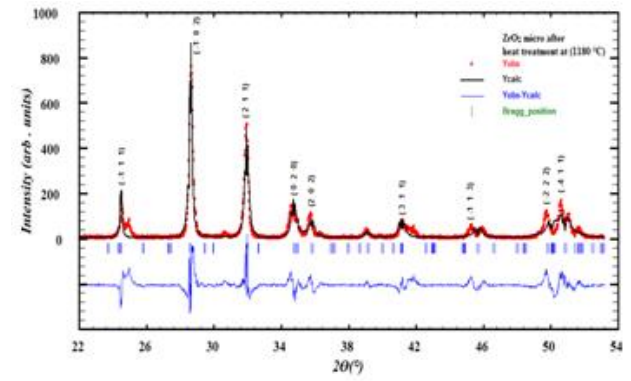

(d)

Figure 2. The refined XRD patterns of (a) ZrO_2 nanopowder, (b) ZrO_2 nanopowder after heat treatment at (1180 °C), (c) ZrO_2 micropowder, (d) ZrO_2 micropowder after heat treatment at (1180 °C). The red line is the experimental data; the blue line is the theoretical data. The lowest trace indicates the difference patterns. The middle vertical lines indicate the peak position.

Table (1) shows unit cell parameters, crystal system, space group and unit cell volume for ZrO_2 (nanopowder before heat treatment, nanopowder after heat treatment, micro powder before heat treatment and micro powder after heat treatment) respectively.

Table 2. Strain and grain size according to Williamson-Hall and grain size according to Debye-Scherrer

Sample	Heat treatment at	D (Williamson-Hall) nm	ε (Williamson-Hall)	D (Scherrer) nm
ZrO_2 nano		23.1	$-125*10^{-5}$	28.6
ZrO_2 nano	1180 °C	36.4	$1*10^{-4}$	34.3
ZrO_2 micro		46.2	$5*10^{-4}$	43.2
ZrO_2 micro	1180 °C	69.3	$-25*10^{-5}$	52.3

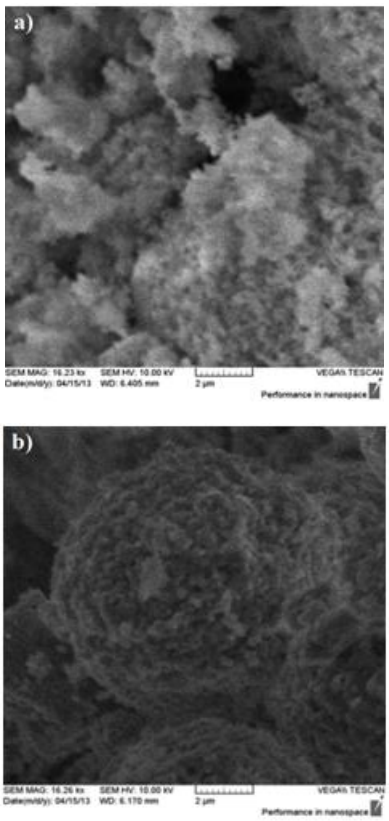

Figure 3. SEM images of ZrO_2 nanopowder: (a) before heat treatment, (b) after heat treatment

Table 1. Unit cell parameters, crystal system, space group and unit cell volume

Samples	Heat treatment at	Unit cell parameter			phase	Space group	Volume ($Å^3$)	angle	
		a	b	c				α= γ	β
ZrO_2 nano		7.962	10.424	6.783	Mono	P2/m	544.619	90	91.859
ZrO_2 nano	1180 °C	13.192	11.754	6.693	Mono	P 2/m	1037.805	90	89.078
ZrO_2 micro		5.313	5.201	5.145	Mono	P2/m	140.621	90	99.233
ZrO_2 micro	1180 °C	7.283	7.283	10.984	Tetra	P 4/m m m	582.691	90	90

From table (1) it can be observed that the unit cell volume for ZrO_2 (nano and micro) powder after heat treatment has increased because of the growth of the crystal. Table (2) shows the strain and the grain size calculated according to Williamson-Hall method and the grain size calculated according to Debye-Scherrer formula for all ZrO_2 under investigation. From table (2) it is observed that the average particle sizes increased after heat treatment. The difference between the grain size calculated according to Williamson-Hall method and the grain size calculated according to Debye-Scherrer formula is attributed to the fact that the Williamson-Hall method takes into account the strain due to the defects and distortions in crystal which contributes to the broadening of the peaks. A negative value for the strain means lattice shrinkage.

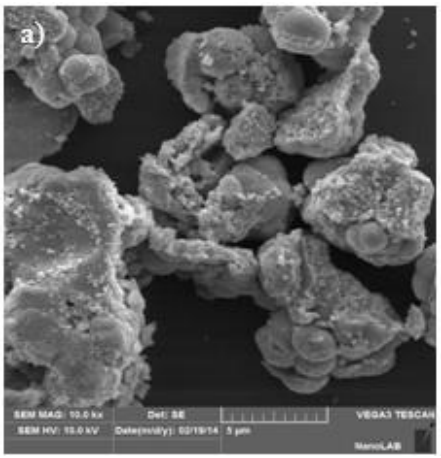

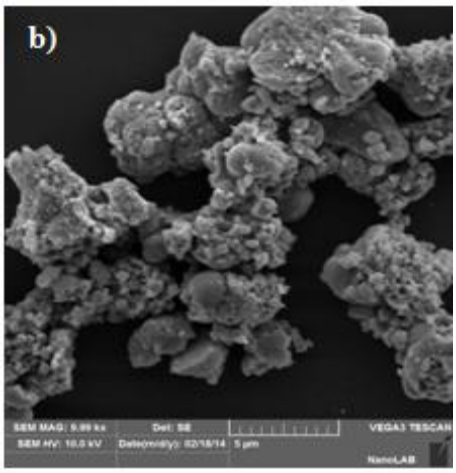

Figure 4. SEM images of ZrO_2 micro powder: (a) before heat treatment, (b) after heat treatment

The SEM micrograph for ZrO_2 nanopowder before heat treatment (Fig. 3a) shows that the particle morphology has homogenous irregular grains. SEM image for ZrO_2 after heat treatment (Fig. 3b) reveals the spherical shape of powder particles. The SEM micrographs for ZrO_2 micro powder before and after heat treatment are shown in figure (4). It is clear that the size of the grains increases after heat treatment.

Conclusions

Qualitative phase analysis has been performed successfully by Rietveld X-ray diffraction using "Fullprof" program for nano and micro powder of ZrO_2 before and after heat treatment at (1180 °C). The obtained results showed a good agreement between the observed X-ray diffraction patterns and that calculated by Rietveld technique. The results show that the grains size estimated by Debye-Scherrer formula and Williamson-Hall formula increases after heat treatment for both the nano and micro ZrO_2 powder. The phase transition from monoclinic (P2/m phase group) to tetragonal (P4/mmm phase group) has been observed for the micro ZrO_2 powder after heat treatment, while no phase transition occurred for the nano ZrO_2 powder. The particles morphology of the ZrO_2 powder before and after heat treatment is identified using SEM. It can be concluded that the Retiveld refinement is more accurate than the comparing method.

REFERENCES

Taylor, M. A., R. E. Alonso, L. A. Errico, A. L´opez-Garc´ıa, P. de la Presa, A. Svane, N. E. Christensen, "Structural, electronic, and hyperfine properties of pure and Ta-doped m-ZrO_2", physical review b, Vol. 85, p.p(1-11), (2012).

Garcia, J. C., L. M. R. Scolfaro, A. T. Lino, V. N. Freire, G. A. Farias, C. C. Silva, H. W. Leite Alves, S. C. P. Rodrigues, E. F. da Silva Jr., "Structural, electronic, and optical properties of ZrO2 frsom ab initio calculations", arXiv:1204.2886v1 [cond-mat.mtrl-sci], (13 Apr 2012).

Al-hazmi, M. H. "Synthesis, characterization and application of zirconia and sulfated zirconia derived from single source precursors", Faculty of the graduate college of the oklahoma state university, (2005).

Buckley, J. "Furnace and refractories" , Refractories and industrial ceramic, Vol. 27, p.p(13), (2006).

Kazemi, F., A. saberi, S. M. Ahmadi, S. Sohrabi, H. R. Rezaie, M. Tahriri, "A novel method for synthesis of met stable tetragonal zirconia nanopowders at low temperatures", Ceramics – Silikáty, Vol. 55, p.p(26-30), (2011).

Gateshki, M., V. Petkov, T. Hyeon , J. Joo, M. Niederberger, Y. Ren, "Interplay between the local structural disorder and the length of structural coherence in stabilizing the cubic phase in nanocrystalline ZrO2", Solid state communications, Vol. 138, p.p(279–284), (2006).

Štefanić, G., S. Musić, "Factors influencing the stability of low temperature tetragonal ZrO2", Croatica chemical acta (CCACAA), Vol. 75, p.p(727-767), (2002).

Piconi, C., G. Maccauro, "Zirconia as a ceramic biomaterial", Biomaterials, Vol. 20, p.p(1 -25), (1999).

Foster, A. S., V. B. Sulimov, F. L. Gejo, A. L. Shluger, R. M. Nieminen, "Structure and electrical levels of point defects in monoclinic zirconia", Physical review b, Vol. 64, p.p(1-10), (2001).

Abbas, H. A., F. F. Hamad, A. K. Mohamad, Z. M. Hanafi, M. Kilo, "Structural properties of zirconia doped with some oxides", Diffusion fundamentals, Vol. 8, p.p(7.1 – 7.8), (2008).

Fabris, S., A. T. Paxton, M. W. Finnis, "A stabilization mechanism of zirconia based on oxygen vacancies only", arXiv:cond-mat/0206080v1 [cond-mat.mtrl-sci], (6 Jun 2002).

Zhu, W., R. Wang, G. Shu, P. Wu, H. Xiao, "First-principles study of the structure, mechanical properties, and phase stability of crystalline zirconia under high pressure", Struct chem, Vol. 23, p.p(601–611), (2012).

Rietveld, H. M. "A profile refinement method for nuclear and magnetic structures", J. appl. cryst., Vol. 2, p.p(65-71), (1969) .

Rietveld, H. M. "Line profiles of neutron powder-diffraction peaks for structure refinement", Acta cryst., Vol. 22, p.p(151-152), (1967).

Smart, L. E., E. A. Moore, "Solid state chemistry 3rd edition", Taylor & Francis group, LLC (2005).

Dinnebier, R. E., K. Friese, "Modern XRD Methods in Mineralogy", in: Introduction to the Mineralogical Sciences, edited by Peter Tropper, in Encyclopedia of Life Support Systems (EOLSS), Developed under the auspices of the UNESCO, Eolss Publishers, Oxford, UK, [http:// www.eolss.net], (2003).

Ståhl, K. "Powder diffraction and the Rietveld method", (2008).

Snellings, R., L. Machiels, G. Mertens, J. Elsen "Rietveld refinement strategy for quantitative phase analysis of partially amorphous zeolitized tuffaceous rocks", Geologica belgica, Vol. 13, p.p (183-196), (2010).

Toby, B. H. "R factors in Rietveld analysis: How good is good enough?", International centre for diffraction data, Vol. 21, p.p(62-70), (2006).

de Oliveira, T. F., R. R. de Avillez, E. K. Epprecht, J. C. B. Queiroz, " Evaluation via multivariate techniques of scale factor variability in the Rietveld method applied to quantitative phase analysis with X-ray powder diffraction", Materials research, Vol. 9, p.p(369-374), (2006).

Karolus, M. "Aplications of Rietveld refinement in Fe-B-Nb alloy structure studies", Proceedings of the 12th scientific international conference "Achievements in mechanical and materials engineering", AMME'2003, Gliwice-Zakopane, p.p(723-726), (2003).

Will, G. "Powder diffraction the Rietveld method and the two stage method to determine and refine crystal structures from powder diffraction data ", Springer, (2005).

Saravanan, R., M. P. Rani, "Metal and alloy bonding - an experimental analysis", Springer, (2012).

Al-Dhahir, T. A. "Quantitative phase analysis for titanium dioxide from X-ray powder diffraction data using the Rietveld method", Diyala journal for pure sciences, Vol. 9, p.p(108-119), (2013).

Mccusker, L. B., R. B. Von Dreele, D. E. Cox, D. LoueËr, P. Scardi, "Rietveld refinement guidelines", J. appl. cryst., Vol.32, p.p(36-50), (1999).

Porob, D. G., T. N. Guru row uru , "Ab initio structure determination via powder X-ray diffraction", Indian academy of sciences, Vol. 113, p.p(435–444), (2001).

Nowosielski, R., R. Babilas, G. Dercz, L. Pająk, "Microstructure of polymer composite with barium ferrite powder", Journal of achievements in materials and manufacturing engineering, JAMME, Vol. 31, p.p(269-274), (2008).

Goforth, R. E., K. T. Hartwig, L. R. Cornwell (auth.), T. C. Lowe, R. Z. Valiev (eds.), "Investigations and applications of severe plastic deformation", Springer-science + Business media dordrecht, (2000).

Mote, VD, Y. Purushotham, BN Dole, "Williamson-Hall analysis in estimation of lattice strain in nanometer-sized ZnO particles", Journal of theoretical and applied physics, Vol. 6, p.p(1-8), (2012).

Zak, A. K., W.H. Abd. Majid , M.E. Abrishami , R. Yousefi, "X-ray analysis of ZnO nanoparticles by Williamson-Hall and size-strain plot methods ", Solid state sciences, Vol. 13, p.p(251-256), (2011).

Rehani, B. R, P B Joshi, K. N Lad, A. Pratap, "Crystallite size estimation of elemental and composite silver nano-powders using XRD principles", Indian journal of pure & applied physics, Vol. 44, p.p(157-161), (2006).

Prabhu, Y. T., K. V. Rao, V. S. Sai Kumar, B. S. Kumari, " X-ray analysis of Fe doped ZnO nanoparticles by Williamson-Hall and size-strain plot", International journal of engineering and advanced technology (IJEAT), Vol. 4, p.p(268-274), (2013).

****